Observation of Longitudinal Acceleration of Electrons Born in a High-Intensity Laser Focus

We have measured the energy and angular distributions of electrons born in and ponderomotively accelerated from a high-intensity laser focus. The angular distribution relative to the $\vec{k}$ of the laser shows the first observation of electrons ejected with momentum in the $\vec{k}$ direction. This forward acceleration comes from the conservation of momentum in the photon field.

At very-high laser intensities, a free electron's oscillatory motion in a laser field becomes anharmonic. A detailed, theoretical examination of electron trajectories and emitted harmonic radiation was conducted by Sarachik and Schappert in 1970.[1] They parameterized the nonlinear electromagnetic wave effects by q (sometimes called η),

$$q^2 = 2\frac{e^2\langle A^2\rangle}{m_0^2c^4}, \tag{1}$$

where c is the speed of light, e and m_0 are the electron charge and rest mass, respectively, ω is the laser frequency, and $\langle A^2\rangle$ is the time average of the square of the vector potential of the laser. When $q < 1$, it is related to the ponderomotive potential (average quiver energy) of the laser, by $\Phi_{\text{pond}} = q^2mc^2/4$. When q approaches 1, a significant drift of the electron in the direction of field propagation arises. This drift, first predicted quantum mechanically in 1964 by Brown and Kibble[2] and classically by Eberly and Sleeper[3] in 1968, is second order in q.

In a laser focus, even at small q, an electron feels a force along the gradient of the ponderomotive potential. At moderate intensities, an electron born in a cylindrically symmetric laser focus with $\mathbf{k}$ in the z direction, is radially accelerated out of the focus.[4,5] An electron gains the full ponderomotive energy if the laser pulse duration τ_L is longer than the time it takes the electron to escape from the laser focus, τ_{esc}. If the laser pulse duration is sufficiently long, the electron's final kinetic energy for linear polarization is equal to its initial energy plus the ponderomotive potential at which it was born.[6] For circular polarization, the electron's final energy is twice its ponderomotive potential due to the conservation of angular momentum in the laser field.[7,8] An electron that is incident on a laser focus can be scattered off the ponderomotive potential, and, in the case of the standing wave, the electron can be Bragg scattered—the Kapitza-Dirac effect.[9] These effects were observed by Bucksbaum *et al.*[10,11] These and all other ponderomotive experiments have examined first-order effects in q and have been conducted with $q << 1$.

References 1–3 assumed that a free electron was initially at rest before the interaction with a plane-wave laser field. In our experiments an electron is released via ionization into the presence of an already intense electromagnetic field. The measurement of electrons with energies exceeding the minimum required for ionization has been labeled above threshold ionization (ATI) and reviewed recently by Freeman and Bucksbaum.[12] Electrons created by ionization are typically released with a few electron volts of energy, which can be considered to be at rest when the ponderomotive potential is much larger. This was observed in experiments by Corkum *et al.*,[7] where $q \sim 0.01$ and the electrons were observed in the radial direction due to their initial drift velocity. Free-electron interactions with laser pulses where q approaches 1 are examined in this experiment. This allows examination of second-order effects in q and, in particular, the predicted longitudinal drift.

The longitudinal drift of an electron was shown by Corkum *et al.*[13] to arise from the absorbed longitudinal momentum that accompanies the energy absorption from the focused laser field. The longitudinal momentum p_z is related to the perpendicular momentum by[13]

$$p_z = \frac{p_\perp^2}{2m_0c}. \tag{2}$$

The perpendicular momentum is related to the total energy by $p_\perp = m_0c\sqrt{2(\gamma-1)}$.[13] Electrons leave the laser focus at an

angle θ with respect to the k vector of the laser given by

$$\theta = \tan^{-1}\sqrt{\frac{2}{\gamma - 1}}. \tag{3}$$

The perpendicular momentum arises from two sources: the conservation of canonical angular momentum[1,14] and the ponderomotive acceleration out of the focus.[2,3]

The longitudinal drift arising from the conservation of angular momentum can be derived from the Hamilton-Jacobi method of Sarachik and Schappert[1] or directly from the invariance of the canonical momentum and energy.[14] If the electron is assumed to be born at $t = 0$ in a field that is uniform in the transverse direction, the electron drift velocity in the nonrelativistic limit, after the laser pulse has passed, is

$$\vec{v}_D = \frac{e}{mc}\vec{A}(0) + \frac{\vec{k}}{|k|}\frac{e^2A^2(0)}{2m^2c^3}. \tag{4}$$

The first term in Eq. (4) represents the transverse drift associated with the conservation of canonical angular momentum; the second term is the associated longitudinal drift. Equation (4) agrees with Eq. (2). If the electron is assumed to be born at the peak of the field, then $A(0) = 0$ for linear polarization, while $|A(0)| = c|E(0)|/\omega$ for circular polarization, where $E(0)$ is the electric field at the time the electron is born.

Reiss[15] and Delone and Krainov[16] have performed detailed calculations of the initial momenta of electrons produced due to the ionization of atoms in strong fields. Both found that for circular polarization the electrons had a forward momentum that was consistent with Eq. (4).

A second radial drift is associated with ponderomotive acceleration out of the laser focus.[2,3] In the weakly relativistic limit, $q < 1$, the radial ponderomotive energy is given by

$$\Phi_p = \frac{e^2\langle A^2\rangle}{2mc^2} = \frac{e^2\langle E^2\rangle}{2m\omega^2}, \tag{5}$$

where $\langle A^2\rangle$ is the temporal average of the square of the vector potential at the time of ionization. Thus for weakly relativistic conditions, an electron born in the focus of a laser pulse will have a final perpendicular velocity

$$v_{\perp r}(\infty) = \left\{\frac{2}{m}\left[\left(\frac{eA(0)}{\sqrt{2}mc^2}\right)^2 + \Phi_{\text{pond}}\right]\right\}^{\frac{1}{2}}\hat{r}. \tag{6}$$

In the above analysis, it is assumed that the laser pulse duration is long enough that the electrons can turn all of the ponderomotive energy into directed kinetic energy.[6] We can combine Eq. (6) with Eqs. (2) and (4) to determine the final drift velocity for circular polarization when $\tau_{\text{esc}} << \tau_L$,

$$\vec{v}_D(\infty) = \sqrt{2}v_{\text{osc}}\hat{r} + \frac{v_{\text{osc}}^2}{c}\hat{z}, \tag{7}$$

and for linear polarization,

$$\vec{v}_D(\infty) = \frac{v_{\text{osc}}}{\sqrt{2}}\hat{r} + \frac{v_{\text{osc}}^2}{4c}\hat{z}. \tag{8}$$

The quiver velocity v_{osc} is defined in terms of the peak electric field (field at ionization),

$$v_{\text{osc}} = \frac{|eE(0)|}{m\omega}. \tag{9}$$

The drift of the electrons is shown schematically in Fig. 59.8.

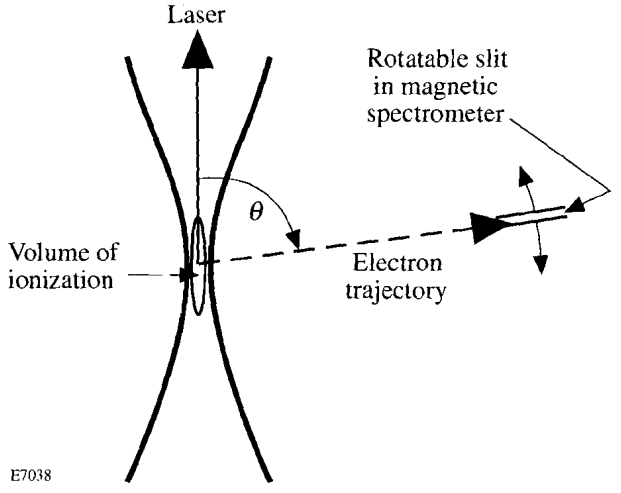

Figure 59.8
Experimental setup showing the position of the magnet gap in the spectrometer in relation to the laser focus, a typical electron trajectory, and the definition of θ. The volume of ionization refers to the volume in which the intensity exceeds the threshold intensity of ionization for a particular charge state and is not to scale.

These results have been confirmed by a fully relativistic Monte Carlo simulation of the electron dynamics. The simulation involved propagating a circularly polarized, Gaussian temporal and spatial profile laser pulse over a few thousand atoms placed at random positions within a laser focus. The laser parameters were based on measurements of the corresponding parameters of our laser system. Electrons were released into the field at the intensity necessary for Coulomb barrier suppression ionization (BSI),[17]

$$E = \frac{\varepsilon_{\text{ion}}^2}{4Z}, \tag{10}$$

where ε_{ion} is the ionization potential and Z is the ionic charge with zero initial velocity. The fully relativistic equation of motion

$$\dot{\vec{p}} = -e\vec{E} - \frac{e}{\gamma mc}\vec{p} \times \vec{B} \tag{11}$$

for the electron trajectories was solved for each electron, and the electrons' positions and velocities after exiting the focus were stored. These electron trajectories, which agreed with Eq. (7), were then convolved with the spectrometer characteristics to give the expected observed energy and angular distributions.

The experiment consisted of creating free electrons via ionization in the laser focus and measuring the ejected electron distributions as a function of energy and angle from the beam axis.

We have constructed a magnetic spectrometer to measure the energy and angular distributions of electrons emitted from a high-intensity laser focus. The spectrometer consists of a magnet for steering the electrons, a scintillator for detection of the electrons, and a photo-multiplier-tube (PMT) for detection of photons created in the scintillator.

The steering magnet is a 10-cm-square piece of high-purity iron with a 6-cm-square cut from the center. A 2-mm gap was cut in one side of the iron, and coils of wire were wrapped around the other three sides of the iron to create an electromagnet. A 100-ms square-topped pulse of voltage is applied across the coils of the magnet resulting in a magnetic field in the gap. The electromagnet is fired 80 ms before the laser pulse, allowing the magnetic field in the gap to be in a steady state by the time electrons are ionized in the laser focus. Residual fields or hysteresis effects on the iron core of the magnet are minimized by degaussing after every firing of the magnet using a slowly diminishing ac current. This technique allows magnetic fields in the gap from 50 to 6000 G to be reliably formed with less than 5% fluctuation from shot to shot.

The magnet is placed above the laser focus with the 2-mm gap aligned with the focus, allowing a line of sight to be traced from the focus through the gap in the magnet. Electrons emitted from the laser focus toward the gap in the magnet enter the gap and are curved by the magnetic field. Electrons with energies giving a gyro-radius of approximately 1.5 cm in the applied magnetic field travel through the gap and strike the scintillator where ultraviolet photons are emitted. The photon flux is then measured using the PMT, and the electrical signal is read by an analog-to-digital converter, which gives a number of counts proportional to the electron number and energy. Peak signal-to-noise ratios of 1000 to 1 are obtained with this setup. The direct line of sight from the focus to scintillator is blocked by 3 cm of aluminum shielding. Aluminum sheet metal is used elsewhere as shielding so that the only possible noise source is stray light through the gap in the magnet.

The energy window of the spectrometer is varied by changing the magnetic field in the gap of the steering magnet. A calibration has been performed using an electron gun producing electrons of known energy. The electron gun was placed at the laser focus and aimed toward the gap in the steering magnet. The magnetic field in the gap was varied by adjusting the voltage applied across the coils of the electromagnet allowing a measurement of the applied voltage versus electron energy. The calibration showed an energy window of $\Delta E/E \sim 0.3$ FWHM. Monte Carlo predictions of the calibration curve are in excellent agreement with the measured calibration.

The angular distribution of electrons in θ (relative to the k of the laser) is measured by rotating the entire spectrometer, which is cylindrically shaped. The central axis of this cylinder passes through the laser focus at 90° to the laser axis. The gap in the magnet is offset from the central axis of the spectrometer and is always aligned so that a clear line of sight can be traced from anywhere on this central axis through the gap in the magnet (see Fig. 59.8).

An angular resolution of ±2° is achieved with this setup. This uncertainty comes from two sources: The first is the geometric angular resolution due to the gap in the magnet. The gap is 2 mm wide, which corresponds to an angular spread of

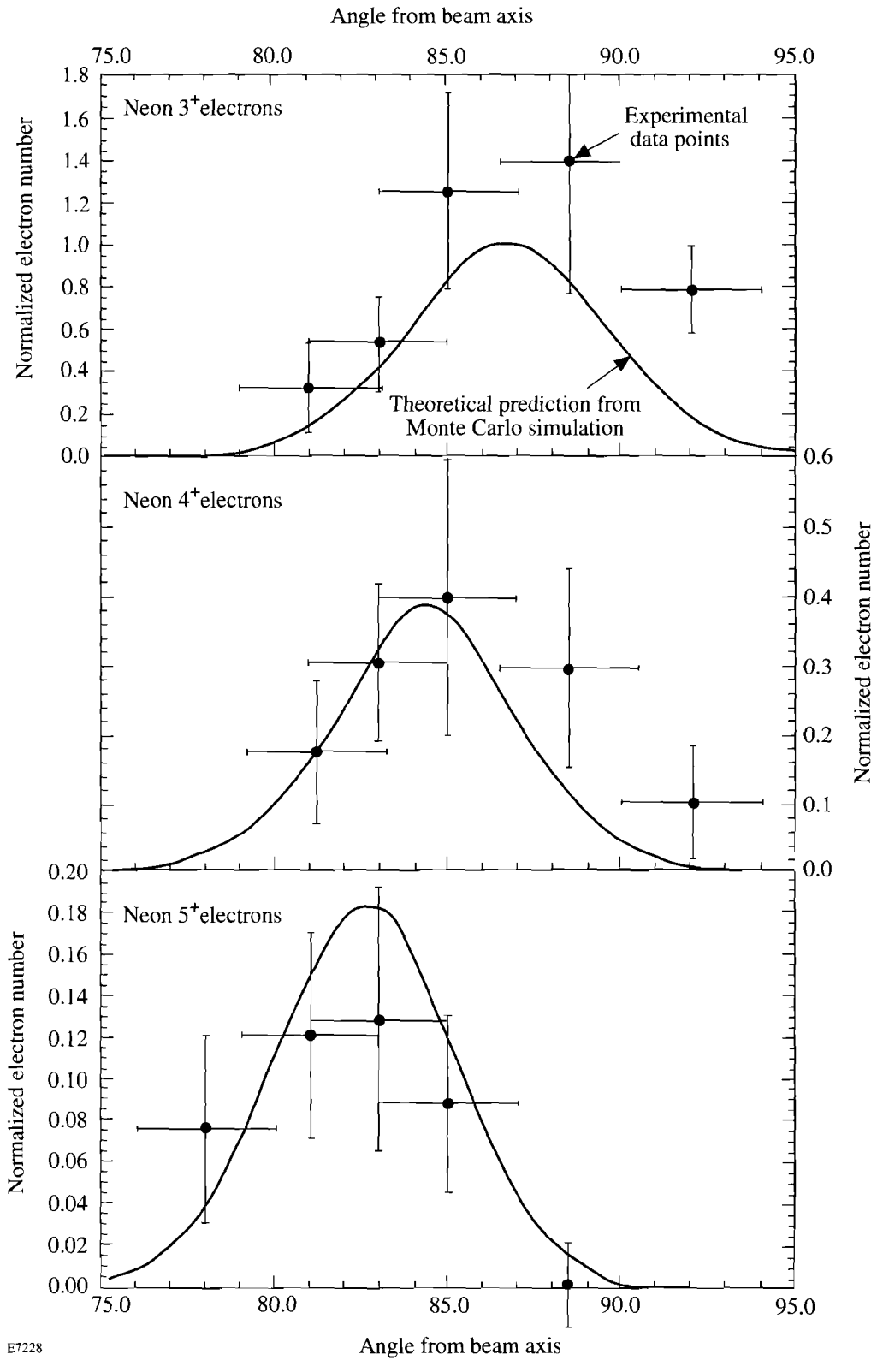

Figure 59.9
Observed experimental angular distribution data points for electrons ionized from the 3^+, 4^+, and 5^+ charge states of neon. The solid curve represents the expected angular distribution for each charge state from the theoretical Monte Carlo simulation of the electron dynamics.

±1° for electrons traveling from the laser focus. The second is due to an asymmetry in the magnetic field of the magnet in the spectrometer. A slight tilt found in the magnetic field deflected electrons by 5°±1° from their original ejection angle. This angle was determined from the detection angle of the Ne^{3+} electron peak on one side of the laser focus compared to its position on the opposite side of the focus. The symmetry of the focus requires that this peak occur at the same angle from the k vector of the laser on both sides of the focus. This was used to determine the angle of electron deflection due to the tilt in the field. This determination is accurate to ±1° and, when combined with the geometric resolving power of the gap, gives a total uncertainty in the angle of ±2°.

The experiments were performed with a 1.05-μm, 1-ps laser system using chirped-pulse amplification (CPA), which is described elsewhere.[18] The experiment discussed in this article was conducted in neon at a pressure of 5×10^{-4} Torr. The laser was focused with $f/6$ optics producing a 5-μm ($1/e^2$ radius) focal spot and a peak laser intensity of approximately 5×10^{17} W/cm^2 ($q \sim 0.5$). Circular polarization was used to avoid possible asymmetries in the electron angular distribution in the plane of polarization upon ionization due to non-zero initial velocities of the electrons along the electric field.[7]

Helium was ionized to confirm the expected ponderomotive energies associated with the BSI threshold intensities. This was accomplished by measuring the energy spectrum of helium and assuming that the highest energy electron peak was from He^{2+}. The energy of this peak was 3.0 kV, which is in agreement with the approximate expected value of 3.5 kV based on BSI in circular polarization and subsequent acceleration of the electron by the ponderomotive potential. Ne^{3+} is created at approximately the same intensity as He^{2+},[17] which was used to determine the electron peaks in the neon spectrum. Energies of the electrons ionized from the 3^+, 4^+, 5^+, and 6^+ charge states of neon were in agreement with the expected ponderomotive energies associated with their corresponding BSI threshold intensities.

Figure 59.9 shows the measured data values of the angular distribution of the 3^+, 4^+, and 5^+ electrons of neon and their expected theoretical positions based on the Monte Carlo simulation. The angular spread in the electron distributions is due primarily to the intensity distribution of the laser focus. The ponderomotive force is linearly related to the gradient of the intensity distribution, which is not always perpendicular to the beam axis in a focused Gaussian beam. As a result some electrons have a small component of ponderomotive acceleration along the beam axis. This acceleration is symmetric about 90° to the beam axis due to the symmetry of a Gaussian beam as it passes through focus and cannot explain any forward shift of the peak of the electron distribution. A normalized electron number is used on the y axis since we do not have an absolute calibration of the number of electrons striking the scintillator in the experiment. A single normalization constant was used in a least-squares fit between the Monte Carlo simulation and experimental data for all three charge states.

Figure 59.10 shows the angle of peak electron number for the 3^+, 4^+, and 5^+ neon charge states measured as a function of electron energy. The points found from the Monte Carlo simulation are in good agreement with the angular distribution predicted in Eq. (3). The experimental points are in good agreement with both of these predicted values. From this we conclude that a nonsymmetric forward acceleration of the electrons has been observed, consistent with the forward drift found in Refs. 1–3.

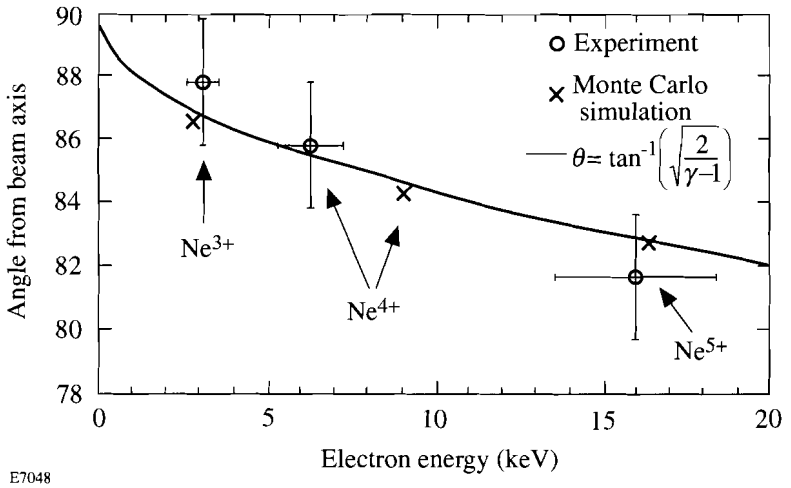

Figure 59.10
Angle of peak electron number for the 3^+, 4^+, and 5^+ electrons of neon from the theoretical Monte Carlo simulation of the electron dynamics and the observed experimental data points. The solid curve is the theoretical prediction of Eq. (4).

We have made the first observations of a forward acceleration of electrons in a high-intensity laser focus. Good agreement is shown between the forward shifted angle of the fully relativistic theoretical predictions and the data obtained.

ACKNOWLEDGMENT

The author's gratefully acknowledge conversations with J. H. Eberly. This work was supported by the U.S. Department of Energy Office of Basic Energy Sciences, Division of Chemical Sciences. Additional support was provided by the U.S. Department of Energy Office of Inertial Confinement Fusion under Cooperative Agreement No. DE-FC03-92SF19460, the University of Rochester, and the New York State Energy Research and Development Authority. The support of DOE does not constitute an endorsement by DOE of the views expressed in this article.

REFERENCES

1. E. S. Sarachik and G. T. Schappert, Phys. Rev. D **1**, 2738 (1970).
2. L. S. Brown and T. W. B. Kibble, Phys. Rev. **133**, A705 (1964).
3. J. H. Eberly and A. Sleeper, Phys. Rev. **176**, 1570 (1968).
4. H. A. H. Boot, S. A. Self, and R. B. R-Shersby-Harvie, J. Elect. Control **4**, 434 (1958).
5. T. W. B. Kibble, Phys. Rev. **150**, 1060 (1966).
6. R. R. Freeman *et al.*, Phys. Rev. Lett. **59**, 1092 (1987).
7. P. B. Corkum, N. H. Burnett, and F. Brunel, Phys. Rev. Lett. **62**, 1259 (1989).
8. P. H. Bucksbaum *et al.*, Phys. Rev. A **41**, 4119 (1990).
9. P. L. Kapitza and P. A. M. Dirac, Proc. Cambridge Philos. Soc. **29**, 297 (1933).
10. P. H. Bucksbaum, M. Bashkansky, and T. J. McIlrath, Phys. Rev. Lett. **58**, 349 (1987).
11. P. H. Bucksbaum, D. W. Schumacher, and M. Bashkansky, Phys. Rev. Lett. **61**, 1182 (1988).
12. R. R. Freeman and P. H. Bucksbaum, J. Phys. B: At. Mol. Opt. Phys. **24**, 325 (1991).
13. P. B. Corkum, N. H. Burnett, and F. Brunel, in *Atoms in Intense Fields*, edited by M. Gavrila (Academic Press, New York, 1992), pp. 109–137.
14. W. B. Mori and T. Katsouleas, Phys. Rev. Lett. **69**, 3495 (1992).
15. H. R. Reiss, J. Opt. Soc. Am. B **7**, 574 (1990).
16. N. B. Delone and V. P. Krainov, J. Opt. Soc. Am. B **8**, 1207 (1991).
17. S. Augst, D. Strickland, D. D. Meyerhofer, S. L. Chin, and J. H. Eberly, Phys. Rev. Lett. **63**, 2212 (1989).
18. Y.-H. Chuang, D. D. Meyerhofer, S. Augst, H. Chen, J. Peatross, and S. Uchida, J. Opt. Soc. Am. B **8**, 1226 (1991).